Available online at www.sciencedirect.com
SCIENCE DIRECT®
PERGAMON
Polyhedron 22 (2003) 1499–1505
POLYHEDRON
www.elsevier.com/locate/poly

Atmospheric pressure chemical vapour deposition of WS_2 thin films on glass

Claire J. Carmalt, Ivan P. Parkin *, Emily S. Peters

Department of Chemistry, Christopher Ingold Laboratories, University College London, 20 Gordon Street, London WC1H 0AJ, UK

Received 28 January 2003; accepted 14 March 2003

Abstract

The atmospheric pressure chemical vapour deposition reaction of $W(CO)_6$, $WOCl_4$ or WCl_6 with $HS(CH_2)_2SH$ or $HSC(CH_3)_3$ at 350–600 °C leads to thin films of WS_2 on glass substrates. The WS_2 films were nanocrystalline, showed a W:S ratio of 1:2 by EDAX and gave Raman bands at 416 and 351 cm^{-1}. The films were silver or gold in colour, adhesive to the substrate and showed Volmer-Webber type growth by SEM. Optical band gaps were 1.4 eV. The films were reflective in the visible region and transparent in the near IR.

Keywords: Metal sulfide; Molecular precursor

1. Introduction

Transition metal disulfides (MS_2) are of interest for many technological applications. They are suitable for use as high-temperature lubricants, hydrogenation catalysts, and high-energy density batteries due to weak van der Waals interactions between adjacent layers in the MS_2 lattice [1–4]. WS_2 thin films have been prepared via dual source chemical vapour deposition (CVD) [5,6], radio frequency sputtering [7], activated reactive evaporation [8], Van der Waals rheotaxy [9], electrodeposition [10], and sulfurisation of WO_3 thin films [11].

Recent research on tungsten sulfide and oxysulfides has focussed on different metal oxidation states for use in micro-batteries. Stoichiometries between $WO_{0.6}S_{1.7}$ and $WO_{2.9}S_{0.5}$ have been produced and lithium intercalation has been successfully performed [12]. Tungsten disulfide (WS_2) has potential use in low cost photovoltaic cells. Ideal materials for use as the absorber material in solar cells should have a band gap of 1–2 eV. WS_2 has a reported band gap of 1.8 eV in the bulk solid and 1.32–1.4 eV in thin film form [2].

Previously WS_2 films have been produced by CVD only using $W(CO)_6$ and H_2S under low pressure CVD conditions [5,6]. This route has the disadvantages of slow growth rates, incomplete substrate coverage and rapid pre-reaction that gives rise to pin-hole defects. In this paper we report WS_2 thin film preparation by atmospheric pressure chemical vapour deposition (APCVD) from a number of tungsten precursors using thiols as the sulfur source.

2. Experimental

Nitrogen (99.99%) was obtained from BOC and used as supplied. Coatings were obtained on SiCO coated glass substrates (SICO is the name given to a barrier layer approximately 50 nm thick that comprises of carbon, silicon and oxygen; the layer is a blocking coating that prevents diffusion of ions from the glass into the film). APCVD experiments were conducted on 90 mm × 45 mm × 4 mm pieces of glass using a horizontal bed cold wall APCVD reactor. The glass was cleaned prior to use by washing with petroleum ether (60–80 °C) and propan-2-ol and then dried in air. A graphite block containing a Whatman cartridge heater was used to heat the glass substrate. The temperature of the substrate was monitored by a Pt–

* Corresponding author. Tel.: +44-207-679-4669; fax: +44-207-679-7463.
E-mail address: i.p.parkin@ucl.ac.uk (I.P. Parkin).

0277-5387/03/$ - see front matter
doi:10.1016/S0277-5387(03)00194-3

Rh thermocouple. The rig was designed so that four separate gas lines could be used. The lines were made of 1/4 in. diameter stainless steel, except for the inlet to the reaction chamber and the exhaust line from the reaction chamber which was 1/2 in. diameter. The nitrogen carrier gas was preheated to 157 °C by being passed along 2 m lengths of coiled stainless steel tubing inside a tube furnace. Gas temperatures were monitored in situ by Pt–Rh thermocouples. Tungsten hexacarbonyl ($W(CO)_6$), tungsten VI chloride (WCl_6) and Tungsten oxychloride ($WOCl_4$) (99.9%, Aldrich Chemical Co.) were used as supplied and placed into a stainless steel bubbler, which was heated by a jacket to 165, 245 and 176 °C, respectively. The vapour produced was introduced into a stream of hot nitrogen that was passed through the bubbler. The sulfur sources used (1,2-ethanedithiol [$HS(CH_2)_2SH$] and 2-methylpropanethiol [$HSC(CH_3)_3$]) were supplied by Aldrich and used without further purification. The sulfur sources were placed in turn in a stainless steel bubbler and heated via a heating jacket ($HS(CH_2)_2SH$, 63 °C; $HSC(CH_3)_3$, 55 °C). The vapour produced was introduced in a stream of hot nitrogen passed through the bubbler. Streams of the tungsten precursor and the sulfur source were mixed by using concentric pipes of 0.25 and 0.5 in. diameter; the inner pipe being 3 cm shorter than the outer pipe. The concentric pipes were attached directly to the mixing chamber of the coater. Gas flows were adjusted using suitable regulators and flow controllers. The exhaust from the reactor was vented directly into the extraction system of a fume cupboard. All of the apparatus was baked out with nitrogen at 150 °C for 30 min before the deposition runs. Suitable two-way and three-way valves (rated at 200 °C) allowed the nitrogen lines to be diverted into or away from the bubbler.

Deposition experiments were conducted by heating the horizontal bed reactor and the bubbler to the required temperatures before diverting the nitrogen line through the bubblers and hence to the reactor. Deposition experiments were timed by stopwatch and routinely lasted 60 s. Whereas WCl_6 used the deposition time of 5 min. At the end of the deposition the bubbler-line was closed and only nitrogen passed over the substrate. The substrate was allowed to cool with the graphite block to approximately 60 °C before it was removed. Coated substrates were handled in air and stored in a dry oxygen free nitrogen atmosphere in a Mbraun Unilab glove box.

Each system was investigated over a range of temperatures from 250 to 600 °C. The large substrates were cut into approximately 40 mm × 10 mm strips for analysis by SEM, XPS, Raman and UV studies. 30 mm × 20 mm strips were used for X-ray diffraction.

X-ray powder diffraction patterns were measured on a Siemens D5000 diffractometer using monochromated Cu $K\alpha_1$ radiation ($\lambda_1 = 1.5406$ Å). The diffractometer used glancing incident radiation (1.5°). Samples were indexed using the Unit Cell software package and compared to database standards. SEM was obtained on a Hitachi S570 instrument and EDXA obtained using the KEVEX system. X-ray photoelectron spectra were recorded using a VG ESCALAB 220i XL instrument using focused (300 μm spot) monochromatic Al Kα radiation at a pass energy of 20 eV. Scans were acquired with steps of 50 meV. A flood gun was used to control charging and the binding energies were referenced to an adventitious C 1s peak at 284.8 eV. Depth profile measurements were obtained by using argon beam sputtering. UV–Vis spectra were recorded in the range 190–1100 nm using a Helios double beam instrument. Reflectance and transmission spectra were recorded between 300 and 1200 nm by a Zeiss miniature spectrometer. Reflectance measurements were standardised relative to a rhodium mirror and transmission relative to air. Band gaps were calculated from the UV spectra. Raman spectra were acquired on a Renishaw Raman System 1000 using a helium–neon laser of wavelength 632.8 nm. The Raman system was calibrated against the emission lines of neon.

The photocatalytic properties of the samples were assessed by the destruction of an overlayer of stearic acid on a 2 cm × 2 cm portion of glass. The sample was pre-irradiated for 1 h at 254 nm using a BDH germicidal lamps (2 × 8 W) prior to the addition of the stearic acid. The stearic acid was applied by dropping 7.5 μl of 0.004 M stearic acid onto the surface of the glass. This was spun at 1500 revolutions per minute to give a thin, even coverage. The coated sample was then irradiated at 15 min intervals for 1 h with intermediate measurement of the IR spectra of the stearic acid overlayer. IR measurements were carried out in the range 3000–2800 cm^{-1}. Film solubility was assessed by immersing a 20 mm × 20 mm piece of coated glass into a solvent (acetonitrile, tetrahydrofuran, dichloromethane, ether, toluene, hexanes and 2 M nitric and hydrochloric acids) for 1 month. Hardness scratch tests were conducted using a brass stylus and a stainless steel scalpel. Film adherence to the glass was assessed using the Scotch tape test. Contact angles for water droplets on the films were calculated by measuring the spread of a known droplet size.

3. Results

APCVD of WS_2 thin films on glass was achieved from dual source reactions where the tungsten precursor was $W(CO)_6$, $WOCl_4$, or WCl_6 and the sulfur source was $HS(CH_2CH_2)SH$ or $HSC(CH_3)$, Table 1. Studies were achieved at substrate temperatures between 300 and 600 °C. No deposition was noted at less than 300 °C. At

Table 1
CVD parameters and film analysis for reaction of $W(CO)_6$, $WOCl_4$ or WCl_6 with $HS(CH_2)_2SH$ or $HSC(CH_3)_3$

Substrate temperature (°C); precursors	Flow conditions sulfur precursor; $TiCl_4$; carrier gas line (l min^{-1})	EDXA	Raman	XRD	Contact angle (°) [a]	Scotch tape test
300; $W(CO)_6$; $HS(CH_2)_2SH$	0.3; 0.5; 2.0	$WS_{1.6}$	WS_2		85	Passed
325; $W(CO)_6$; $HS(CH_2)_2SH$	0.3; 0.5; 2.0	$WS_{1.7}$	WS_2		80	Passed
350; $W(CO)_6$; $HS(CH_2)_2SH$	0.3; 0.5; 2.0	$WS_{1.6}$	WS_2		75	Passed
350; $W(CO)_6$; $HS(CH_2)_2SH$	0.2; 0.6; 2.0	$WS_{1.8}$	WS_2		60	Passed
350; $W(CO)_6$; $HS(CH_2)_2SH$	0.4; 0.4; 2.0	$WS_{2.0}$	WS_2		9	Passed
375; $W(CO)_6$; $HS(CH_2)_2SH$	0.3; 0.5; 2.0	$WS_{1.9}$	WS_2		82	Passed
400; $W(CO)_6$; $HS(CH_2)_2SH$	0.3; 0.5; 2.0	$WS_{1.5}$	WS_2	Nanocrystalline WS_2	57	Passed
450; $W(CO)_6$; $HS(CH_2)_2SH$	0.3; 0.5; 2.0	$WS_{1.8}$	WS_2		84	Passed
500; $W(CO)_6$; $HS(CH_2)_2SH$	0.3; 0.4; 1.0	$WS_{1.8}$	WS_2		40	Failed
600; $W(CO)_6$; $HS(CH_2)_2SH$	0.3; 0.5; 2.0	$WS_{1.7}$	WS_2		6	Failed
275; $WOCl_4$; $HS(CH_2)_2SH$	0.3; 2.0; 2.0	$WS_{1.5}$	WS_2		58	Passed
300; $WOCl_4$; $HS(CH_2)_2SH$	0.3; 2.0; 2.0	$WS_{2.0}$	WS_2		48	Passed
350; $WOCl_4$; $HS(CH_2)_2SH$	0.3; 2.0; 2.0	$WS_{1.7}$	WS_2		38	Passed
350; $WOCl_4$; $HS(CH_2)_2SH$	1.3; 1.0; 2.0	$WS_{2.2}$	WS_2		74	Passed
350; $WOCl_4$; $HS(CH_2)_2SH$	1.3; 1.3; 1.7	$WS_{1.8}$	WS_2		28	Passed
400; $WOCl_4$; $HS(CH_2)_2SH$	0.3; 2.0; 2.0	$WS_{1.9}$	WS_2		9	Failed
450; $WOCl_4$; $HS(CH_2)_2SH$	0.3; 2.0; 2.0	$WS_{1.8}$	WS_2		17	Failed
275; WCl_6; $HS(CH_2)_2SH$	0.3; 2.0; 2.0	$WS_{1.1}$	WS_2		43	Passed
300; WCl_6; $HS(CH_2)_2SH$	0.3; 2.0; 2.0	$WS_{2.0}$	WS_2		63	Passed
350; WCl_6; $HS(CH_2)_2SH$	0.3; 2.0; 2.0	$WS_{2.3}$	WS_2		66	Passed
350; WCl_6; $HS(CH_2)_2SH$	1.3; 2.0; 1.0	$WS_{2.1}$	WS_2		73	Passed
350; WCl_6; $HS(CH_2)_2SH$ [b]	0.3; 2.0; 2.0	$WS_{1.9}$	WS_2	Nanocrystalline WS_2	100	Failed
400; WCl_6; $HS(CH_2)_2SH$	0.3; 2.0; 2.0	$WS_{2.3}$	WS_2		60	Passed
450; WCl_6; $HS(CH_2)_2SH$	0.3; 2.0; 2.0	$WS_{2.0}$	WS_2		54	Failed
500; WCl_6; $HS(CH_2)_2SH$	0.3; 2.0; 2.0	$WS_{1.9}$	WS_2		–	Failed
350; WCl_6; $HSC(CH_3)_3$	1.3; 2.0; 1.0	$WS_{2.0}$	WS_2		82	Passed
400; WCl_6; $HSC(CH_3)_3$	0.3; 2.0; 2.0	$WS_{2.1}$	WS_2		93	Passed
450; WCl_6; $HSC(CH_3)_3$	0.3; 2.0; 2.0	$WS_{1.9}$	WS_2		103	Passed
300; $WOCl_4$; $HSC(CH_3)_3$	0.3; 2.0; 2.0	$WS_{1.5}$	WS_2		100	Passed
400; $WOCl_4$; $HSC(CH_3)_3$	0.3; 2.0; 2.0	$WS_{1.8}$	WS_2		95	Passed
500; $WOCl_4$; $HSC(CH_3)_3$	0.3; 2.0; 2.0	$WS_{1.9}$	WS_2		82	Passed
275; $W(CO)_6$; $HSC(CH_3)_3$	0.3; 0.5; 2.0	$WS_{1.9}$	WS_2		57	Passed
300; $W(CO)_6$; $HSC(CH_3)_3$	0.3; 0.5; 2.0	$WS_{1.9}$	WS_2		43	Passed
300; $W(CO)_6$; $HSC(CH_3)_3$	1.0; 0.8; 1.0	$WS_{2.0}$	WS_2		73	Passed
350; $W(CO)_6$; $HSC(CH_3)_3$	0.3; 0.5; 2.0	$WS_{1.4}$	WS_2		60	Passed
400; $W(CO)_6$; $HSC(CH_3)_3$	0.3; 0.5; 2.0	$WS_{0.9}$	WS_2		50	Failed
500; $W(CO)_6$; $HSC(CH_3)_3$	0.3; 0.5; 2.0	$WS_{1.3}$	WS_2		39	Failed
600; $W(CO)_6$; $HSC(CH_3)_3$	0.3; 0.5; 2.0	$WS_{2.0}$	WS_2		33	Failed

[a] Contact angle for glass with no film deposited measured at 40–60°.
[b] Annealed at 600 °C under $HS(CH_2)_2SH$ for 30 min directly after deposition.

temperatures above 500 °C the coating was localised towards the front of the substrate.

The WS_2 films were reflective and were either silver or gold in colour dependent on film thickness. The films were generally adhesive to the glass substrate and in most cases passed the Scotch tape test. They could be scratched with a brass stylus and with a steel scalpel. The films were surprisingly robust to a wide range of common solvents (water, acetone, toluene, acetonitrile) and dilute mineral acids (hydrochloric) in that they showed no visible change on 1 month of immersion. The films did dissolve in dilute nitric acid after a week of immersion.

Scanning electron microscopy showed that each film grew via a Volmer-Webber type mechanism, Fig. 1. Typically each film consisted of a 'crazy-paving' patchwork of WS_2 particles of size 200 nm. Edge-on SEM photographs enabled a determination of film thickness and indicated a typical growth rate of 400 nm min^{-1}. Energy dispersive X-ray analysis showed that the films were composed of tungsten and sulfur with elemental ratios close to 1:2. Compositions for the various films are listed in Table 1. Some slight deviations were noted from this composition however this tended to be for the thinner films grown at lower temperatures where breakthrough to the underlying glass was extensive and

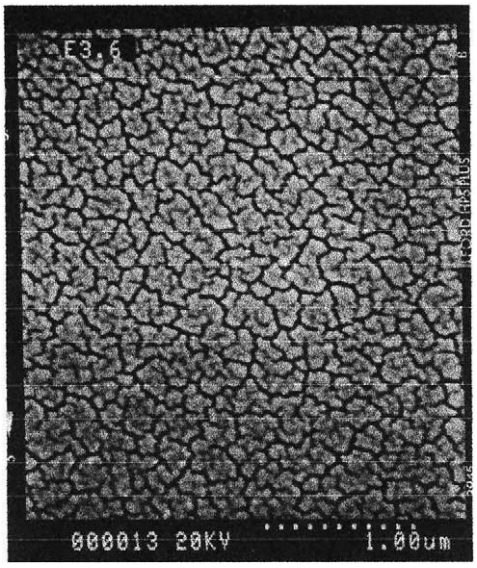

Fig. 1. Scanning electron microscopy image of the film prepared from the APCVD of $WOCl_4$ and $HS(CH_2)_2SH$ at 275 °C.

interfered with accurate composition analysis. In any case the EDAX composition is accurate to ±0.1. No evidence for carbon, oxygen or chlorine contamination was noted to the detection limits of the instrument.

X-ray photoelectron spectroscopy was consistent with the formation of WS_2 thin films. The surface showed the presence of a partly oxidised tungsten oxide over-layer, however this was readily removed on depth profiling using argon to leave the bulk of the film consisting of just W and S. The films appeared slightly sub-stoichiometric in sulfur—thus agreeing with the EDAX results. The W $4f_{7/2}$ and W $4f_{5/2}$ peaks were observed in all samples at 33.6 and 31.4 eV and the S 2p peak was observed at 162.2 eV. This compares very well with W 4f peaks (33.6 and 31.4 eV) and S 2p (162.0 eV) peaks for WS_2 films prepared by solid state annealing [11]. No evidence was seen for incorporation of chlorine in the films. A very small amount of carbon was noted in the first surface scan of each XPS measurement and comes from surface contamination in the XPS instrument (residual carbon background from pump oil) or from exposure of the samples to the atmosphere. The carbon concentration was reduced to detection limits on the first sputtering of the surface.

The Raman spectra were very diagnostic and indicated that in every experiment single phase WS_2 had been deposited, Fig. 2. The principle bands observed in the Raman were at 351 and 416 cm^{-1}. These correspond to first order Raman peaks. The band at 351 cm^{-1} is assigned as an E_{2g} mode for motion of W+S in the x–y plane and the band at 416 cm^{-1} assigned as an A_{1g} mode for the motion of two S atoms along the z-axis of the unit cell [6]. The smaller peaks observed at 178, 232, 297, 387, 483, 526, 584 and 702 cm^{-1} have been assigned to second order Raman peaks that arise from phonon couplings with a nonzero momentum [6]. The position and intensity of all of the first and second order Raman bands match extremely well with single crystal 2H–WS_2 and with thin film WS_2. Previous Raman measurements on WS_2 thin films have shown that the exact position of the E_{2g} band and the full width half height maximum of the A_{1g} band can be related to the orientation of the WS_2 film relative to the substrate [6]. A comparison with the spectra obtained in this work indicates that the CVD prepared crystallites are arranged in a random orientation with crystallites both perpendicular and parallel to the substrate.

The X-ray diffraction patterns showed either an amorphous ill-defined pattern or one that corresponded to nanocrystalline WS_2, Fig. 3. The most crystalline pattern was obtained by taking the film deposited from WCl_6 and $HS(CH_2)_2SH$ at 350 °C and annealing it at 600 °C for 30 min under a flow of $HS(CH_2)_2SH$. However even under these circumstances line-broadening studies (Scherrer equation based on (0 0 4) of WS_2 [13]) indicated a crystallite size of 25 nm. One literature report suggests that thin film WS_2 can only be properly crystallised at temperatures in excess of 700 °C [11]. This was not possible in this study as the substrate is glass and softens at 650 °C.

The contact angle for water droplets on the WS_2 films prepared by CVD showed a wide variation. Most of the films had contact angles in excess of 50°—indicating that the films are hydrophobic. Contact angles for water droplets on the uncoated substrate were typically 40°–60°. However some films had very low contact angles between 6 and 10° indicating a degree of hydrophilicity. This low contact angle is almost certainly associated with a high porosity within the films rather than some form of photo-induced hydrophilicity as the contact angles did not change upon photo-irradiation—as they would do for a photo-active film such as TiO_2 [14]. The contact angle data was such that useful parallels between contact angle and deposition conditions could not be drawn. The WS_2 films did not show any measurable photo-activity for the destruction of a stearic acid over-layer when using 254 nm radiation.

An optical band gap of 1.4 eV was measured for the WS_2 films from a Tauc plot. There was little variation in the band gap between samples. This band gap compares extremely favourably with thin film WS_2 made by solid state reaction that had a band gap of 1.42 eV [11], and single crystal 2H–WS_2 that had a value of 1.3 eV [15].

The reflectance/transmission profile for the WS_2 films from 400 to 3000 nm is shown in Fig. 4. This shows that the films are transparent in the visible and far IR regions. It also shows that the films are reflective in the visible. This correlates with the appearance of the films, which act as conventional mirrors.

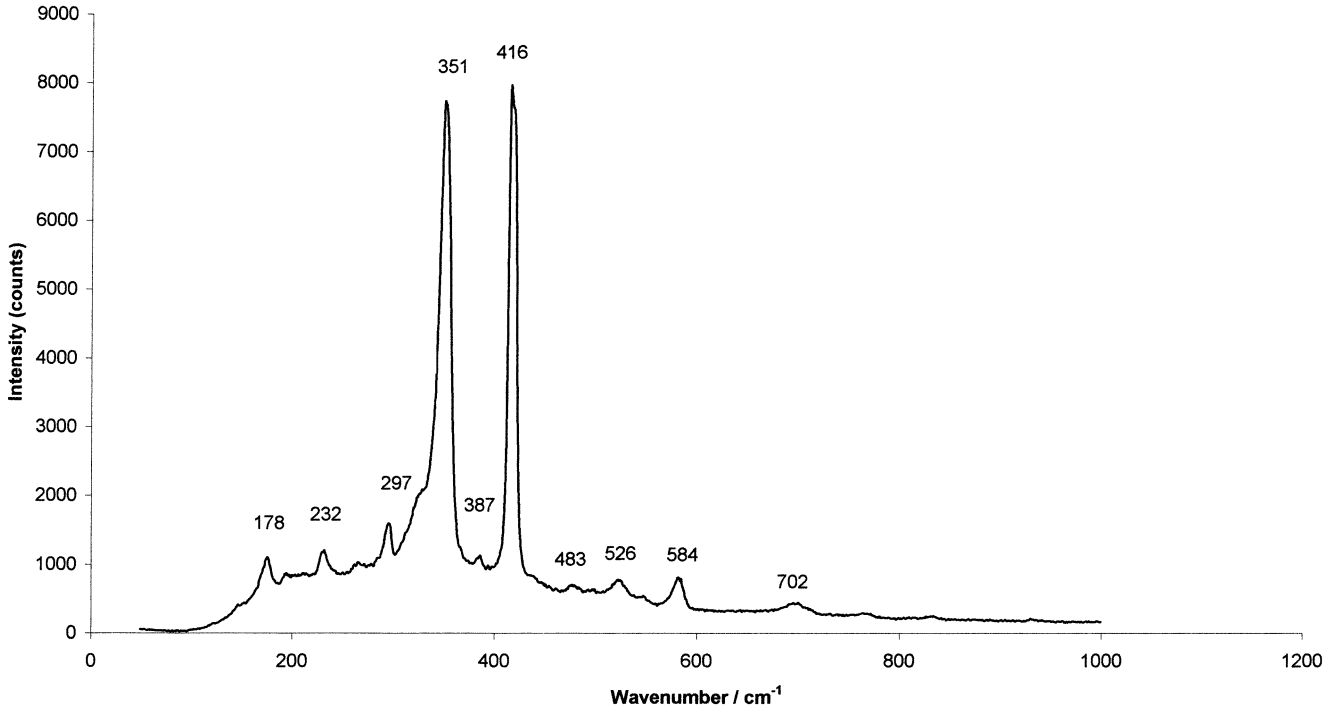

Fig. 2. Raman spectrum of a WS_2 film deposited on glass from $WOCl_4$ and $HSC(CH_3)_3$ at 300 °C.

The electrical conductivity of the films is in the range of 0.1–1.0 Ω^{-1} m^{-1}. This correlates very well with previous thin film measurements and indicates that the material is a semiconductor and that the conductivity is mainly limited by grain boundary effects [16]. This also correlates with the SEM images (Fig. 1) which shows definite gaps between the islands of film growth.

4. Discussion

The dual source APCVD reaction of volatile tungsten reagents and $HS(CH_2)_2SH$ or $HSC(CH_3)_3$ forms thin films of WS_2 on glass substrates. All films had the same shiny reflective appearance irrespective of the precursors used. The temperature required for the onset of deposi-

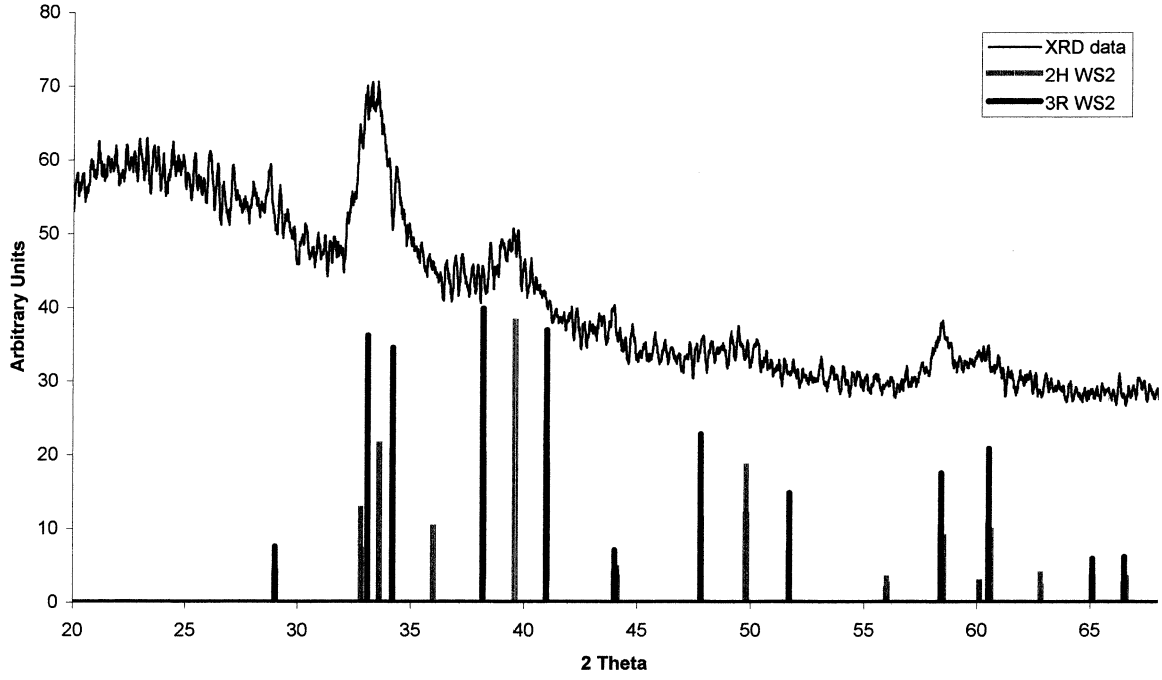

Fig. 3. X-ray powder diffraction pattern for WS_2 film produced from the APCVD reaction of WCl_6 and $HS(CH_2)_2SH$ at 350 °C and annealed at 600 °C for 30 min under $HS(CH_2)_2SH$. Bottom trace represents the powder diffraction pattern for the 2H–WS_2 standard.

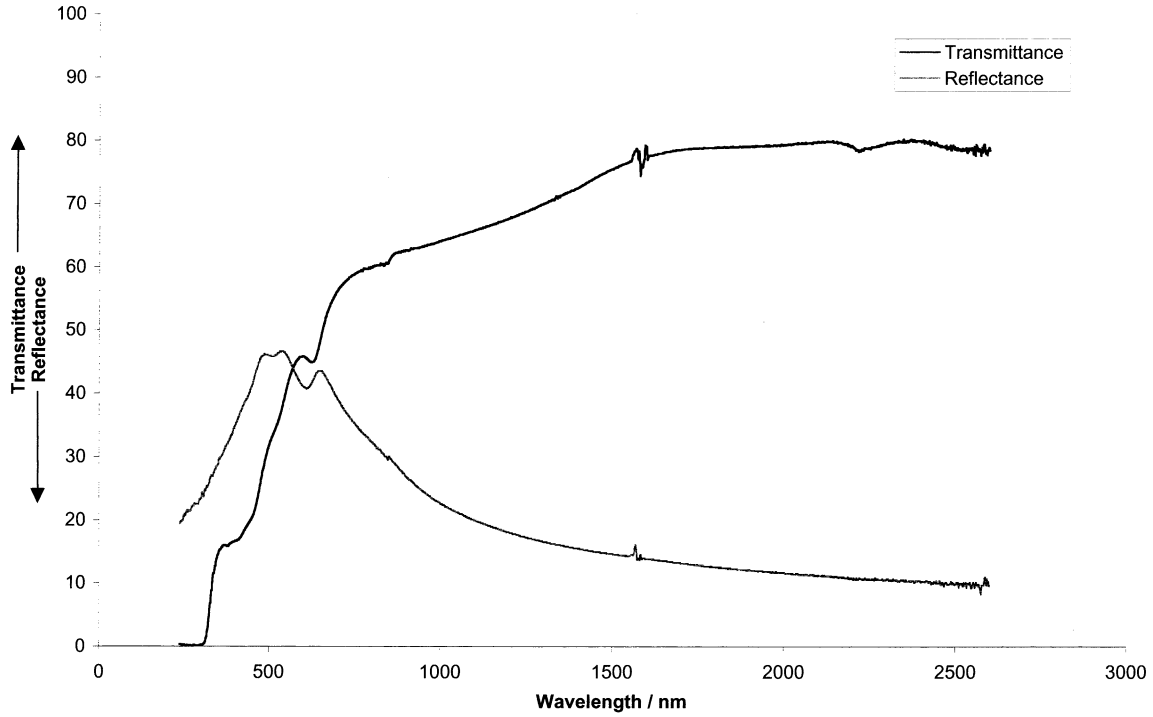

Fig. 4. Reflectance/transmission plot for WS_2 film prepared from the APCVD reaction of $WOCl_4$ and $HSC(CH_3)_3$ at 500 °C.

tion showed remarkably little variation on precursor. Typically substrate temperatures below 300 °C were too low to initiate CVD. Deposition was noted at all substrate temperatures from 350 to 600 °C with all precursors. At substrate temperatures of 350–450 °C the WS_2 films covered the whole of the substrate, however at higher temperatures the deposition was localised more towards the front edge of the substrate, such that at 600 °C only the front 2–3 cm were covered. This deposition pattern is consistent with fast surface reactivity at high temperature such that the precursor gas stream is depleted so rapidly that the deposition is localised only at the front of the substrate-in effect the deposition process is mass transport limited.

The mechanism for the deposition processes was not looked into. However, despite using metal chloride precursors no chlorine was detected in the film. This indicates that a clean decomposition pathway is available, most probably by elimination of HCl with concomitant formation of W–S bonds. Surprisingly $WOCl_4$ proved to be an effective precursor and did not form tungsten oxysulfide coatings. Our initial thoughts were that this precursor, with a built in strong tungsten oxygen double bond, would provide oxygen for the film and hence form an oxysulfide. The fact that this was not observed indicates that the oxygen is lost in the CVD process. A further notable point is that despite using precursors containing carbon, no carbon was found in the films.

The Raman spectra of all of the films correspond to patterns of WS_2 crystal growth that are aligned in a random fashion relative to the surface. It has been shown previously that the relative intensity and width of the Raman peaks at 420 and 350 cm^{-1} of WS_2 can be related to preferred growth orientation of WS_2 parallel or perpendicular to the surface [11]. The ratios for the E_{2g}/A_{1g} bands are similar to those reported in the literature for 2H–WS_2 rather than 3R–WS_2, which is largely consistent with the XRD data (ICCD 08-0237 for 2H–WS_2 and ICCD 35-0651 for 3R–WS_2). Fig. 3 shows that the patterns for 2H and 3R WS_2 are extremely similar. The peaks obtained in this study are slightly broader than for polycrystalline films with single orientation parallel or perpendicular to the substrate. [11]. This indicates a more disordered random arrangement of the WS_2.

Surprisingly in all of the deposition experiments single phase WS_2 was observed. A number of W–S phases are known including WS_3 and WS_2 polytypes. The films formed in this study correspond best with the 2H–WS_2 polytype. Varying the gas flows through the bubblers such that excess tungsten or thiol was used in the experiment did not seem to have an effect on the phase of tungsten sulfide formed.

Previously WS_2 thin films have been laid down by low pressure CVD from reaction of $W(CO)_6$ and H_2S [11]. Growth rates in these reactions were of the order of 20–25 nm min^{-1}. This is significantly less than that obtained from the APCVD reactions reported here ($\approx$ 400 nm min^{-1}). The onset temperature for deposition with H_2S was 300 °C [11] and somewhat comparable to that observed here (300–350 °C). The reactions with

H_2S produced thin films of WS_2 which were composed of plate like crystallites agglomerated together to form a film. Use of thiols, as reagents, produces a more uniform and less crystalline film than use of H_2S. This is probably a result of the faster growth kinetics employed in the APCVD technique, where multiple nucleation sites are generated for film growth. The APCVD films are also less well ordered than the comparable films formed using $W(CO)_6$ and H_2S in relation to the substrate where preferential growth parallel to the surface were common. Thiols, although malodorous, do not have the same level of extreme toxicity as H_2S. The films generated from thiols also do not shown pinhole defects associated with gas phase reaction which can be a problem with the use of H_2S [17]. We have also shown that despite varying the tungsten and sulfur source provided the reagents are combined at sufficiently elevated temperatures only WS_2 is formed over a variety of reagent concentrations. This indicates that WS_2 is the thermodynamic product in this system.

5. Conclusions

APCVD offers a facile method for the deposition of WS_2 thin films on glass. The WS_2 films are randomly orientated and made up of nanocrystallites. The films are silver or gold in appearance and are free of contamination with carbon, oxygen and chlorine (to detection limits ≈ 0.5 at.%). Notably a wide range of tungsten precursors can be utilised in the APCVD process. We have further shown the utility of using thiols as a somewhat less toxic alternative to H_2S as a sulfur source.

Acknowledgements

I.P.P. thanks the EPSRC for grant GR/M82592 for purchase of the Renishaw Raman microscope. E.P. thanks the EPSRC for a studentship.

References

[1] M.S. Whittingham, Prog. Solid State Chem. 12 (1978) 41.
[2] K. Ellmer, C. Stock, K. Diesner, I. Sieber, J. Cryst. Growth 182 (1997) 389.
[3] J. Cheon, J.E. Gozum, G.S. Girolami, Chem. Mater. 9 (1997) 1847.
[4] S.D. Jones, J.R. Akridge, J. Power Sources 54 (1995) 63.
[5] W.K. Hoffman, J. Mater. Sci. 23 (1988) 3981.
[6] J.W. Chung, Z.R. Dai, F.S. Ohuchi, J. Cryst. Growth 186 (1988) 137.
[7] (a) M. Genut, L. Margulis, R. Tenne, G. Hodes, Thin Solid Films 219 (1992) 30;
(b) M. Regula, C. Ballif, J.H. Moser, F. Levy, Thin Solid Films 280 (1996) 67;
(c) D. Tonti, F. Varsano, F. Decker, C. Ballif, M. Regula, M. Remskar, J. Phys. Chem. B 101 (1997) 2485;
(d) C. Ballif, M. Regula, P.E. Schmid, M. Remskar, R. Sanjines, F. Levy, Appl. Phys. A 62 (1996) 543;
(e) I. Martin-Litas, P. Vinatier, A. Levasseur, J.C. Dupin, D. Gonbeau, F. Weill, Thin Solid Films 416 (2002) 1.
[8] A. Klein, S. Tiefenbacher, V. Eyert, C. Pettenkofer, W. Jaegermann, Phys. Rev. B 64 (2001) 205416.
[9] T. Tsirlina, S. Cohen, H. Cohen, L. Spair, M. Peisach, R. Tenne, A. Matthaeus, S. Tiefenbacher, W. Jaegermann, E.A. Ponomarev, C. Levy-Clement, Sol. Energy Mater. 44 (1996) 457.
[10] J.J. Devadasan, C. Sanjeeviraja, M. Jayachandran, J. Cryst. Growth 226 (2001) 67.
[11] S.J. Li, J.C. Bernede, J. Pouzet, M. Jamali, J. Phys.: Condens. Matter 8 (1996) 2291.
[12] (a) R.A. Scott, A.J. Jacobson, R.R. Chianelli, W.H. Pan, E.I. Stiefel, K.O. Hodgson, S.P. Cramer, Inorg. Chem. 25 (1986) 1461;
(b) G.F. Khudorozhko, I.P. Asanov, L.N. Mazalov, E.A. Kravtsova, G.K. Parygina, V.E. Fedorov, J.E. Mironov, J. Electron Spectrosc. Relat. Phenom. 68 (1994) 199.
[13] H.P. Klug, L.E. Alexander, X-ray Diffraction Procedure for Polycrystalline and Amorphous Materials, second ed., Wiley, New York, 1974.
[14] A. Mills, S.K. Lee, A. Lepre, I.P. Parkin, S.A. O'Neill, Photochem. Photobiol. Sci. 1 (2002) 865.
[15] A.R. Beal, W.Y. Liany, H.P. Hughes, J. Phys. C: Solid State Phys. 9 (1976) 2449.
[16] E. Gourmelon, O. Ligner, H. Hadouda, G. Couturier, J.C. Bernede, J. Tedd, J. Pouzet, J. Salardenne, Solar Energy Mater. Solar Cells 46 (1997) 115.
[17] L. Price, Ph.D. Thesis, University of London, 2001.